MEDICAL SCIENCE MONITOR

ANIMAL STUDY

e-ISSN 1643-3750
© Med Sci Monit, 2020; 26: e927458
DOI: 10.12659/MSM.927458

Received: 2020.07.15
Accepted: 2020.08.18
Available online: 2020.08.20
Published: 2020.08.26

Effect of Sleeve Gastrectomy on Glycometabolism via Forkhead Box O1 (FoxO1)/Lipocalin-2 (LCN2) Pathway

Authors' Contribution:
Study Design A
Data Collection B
Statistical Analysis C
Data Interpretation D
Manuscript Preparation E
Literature Search F
Funds Collection G

ACEFG 1 Zhi Liu
BCD 2 Fuyun Sun
BCD 2 Zitian Liu
BCD 1 Xiaoyang Wang
DEF 1 Mingxin Jin
E 1 Jiajia Mao
BC 1 Qunzheng Wu
BCD 2 Shaohua Yan
E 2 Kai Xu
AEFG 1 Kexin Wang
AF 3 Sanyuan Hu

1 Department of General Surgery, Qilu Hospital, Cheeloo College of Medicine, Shandong University, Jinan, Shandong, P.R. China
2 Cheeloo College of Medicine, Shandong University, Jinan, Shandong, P.R. China
3 Department of General Surgery, Shandong Qianfoshan Hospital, Cheeloo College of Medicine, Shandong University, Jinan, Shandong, P.R. China

Corresponding Author: Kexin Wang, e-mail: wkxqlyy201407@yeah.net

Source of support: This study was financially supported by the National Natural Science Foundation of China (Grant No. 81873650), the Shandong Medical and Health Technology Development Project (Grant No. 2014WS0148) and the Qilu Hospital of Shandong University Scientific Research Fund (Grant No. 2019QLQN08)

Background: The mechanism by which sleeve gastrectomy (SG) improves glycometabolism has remained unclear so far. Increasing evidence has demonstrated that bone is a regulator of glucose metabolism, and osteoblast-derived forkhead box O1 (FoxO1) and lipocalin-2 (LCN2) are regulators of energy metabolism. The aim of this study was to investigate whether the FOXO1/LCN2 signaling pathway is involved in the anti-diabetic effect of SG.

Material/Methods: Insulin resistance was induced in Wistar rats, which were then intraperitoneally injected with streptozotocin to induce a type 2 diabetic state. Levels of fasting blood glucose, serum insulin, HbA1c, and LCN2 were analyzed at corresponding time points after SG and sham surgeries. The expressions of FOXO1, LCN2, and the melanocortin 4 receptor (MC4R) in bone and hypothalamus were detected by immunofluorescence. FOXO1 siRNA was applied to downregulate FOXO1 expression in osteoblasts of rats. The influence of FOXO1 gene on expression of LCN2 was investigated in cultured osteoblasts by western blot and PCR.

Results: Glucose metabolism in the SG group was significantly improved. The LCN2 expression in bone in the SG group was higher than that in the sham group, whereas FOXO1 expression in the SG group was lower than that in the sham group. The binding rate of LCN2 and MC4R in the hypothalamus was also higher in the SG group compared with that in the sham group. The downregulation of FOXO1 expression in osteoblasts was accompanied by upregulation of LCN2 expression.

Conclusions: These results suggest that the FOXO1/LCN2 signaling pathway participates in the anti-diabetic effect of SG.

MeSH Keywords: Bariatric Surgery • Forkhead Transcription Factors • Glycomics • Lipocalin 1 • Receptor, Melanocortin, Type 4

Full-text PDF: https://www.medscimonit.com/abstract/index/idArt/927458

Indexed in: [Current Contents/Clinical Medicine] [SCI Expanded] [ISI Alerting System] [ISI Journals Master List] [Index Medicus/MEDLINE] [EMBASE/Excerpta Medica] [Chemical Abstracts/CAS]

Background

Diabetes mellitus (DM) jeopardizes human health and is associated with high disability and mortality rates [1]. Type 2 diabetes mellitus (T2DM) features disrupted glycometabolism, largely due to insulin resistance (IR) in target tissue [2]. Among the therapies of DM, metabolic surgery can significantly reduce the weight of patients and improve glycometabolism. A meta-analysis showed that the cure rate and remission rate of diabetes mellitus after metabolic surgery are 78.1% and 86.6%, respectively [3]. At present, 2 of the most widely used metabolic surgeries are sleeve gastrectomy (45.9%) and Roux-en-Y gastric bypass (39.6%) [4]. SG surgery not only has a remarkable effect on reducing weight and improving glycometabolism, but also has the advantages of relatively simple surgery process and fewer complications. In recent years, SG surgery has become the first choice of metabolic surgery [5]. However, the mechanism by which metabolic surgery improves glycometabolism has remained unclear. In the past, it was believed that the liver was the main organ for glycogen storage and the trigger for circulating glucose flow [6]. Skeletal muscle plays an important role in the body's energy metabolism balance and insulin resistance process, and over 80% of glucose uptake and consumption occurs via skeletal muscles. However, recent studies have found that the glucose absorption of the femur, fibula, tibia, and even the skull is higher than traditionally believed to occur in muscle and fat tissue [7,8]. In recent years, studies have found that bone can exhibit the characteristics of endocrine organs, which means they can secrete multiple hormones to participate in the systemic endocrine cycle [9–11]. The surface of osteoblasts contains insulin receptors. Therefore, when insulin increases in the body, it can directly stimulate osteoblasts and promote the synthesis and secretion of collagen and bone matrix. Insulin deficiency can reduce the number and activity of osteoblasts and affect bone formation. Thus, some scholars put forward the theory of a bone-pancreatic endocrine feedback loop [7,10]. Lipocalin 2 (LCN2), secreted by osteoblasts, is the latest hormone discovered that has important regulatory functions for energy metabolism.

LCN2, a protein known as neutrophil gelatinase-associated lipocalin, is expressed in various tissues such as immune cells, adipose tissue, and kidney, and is implicated in diseases associated with inflammation and obesity and T2DM. Furthermore, LCN2 also acts as a bone-derived lipid carrier protein, and is mainly enriched in osteoblasts. LCN2 can increase insulin release to improve glycometabolism. LCN2 can pass through the blood-brain barrier and act on the melanocortin 4 receptor (MC4R) in the hypothalamus, thus activating the MC4R-dependent anorexia pathway, and then affecting appetite and regulating liver glycogen output [12]. Some studies showed that forkhead box O1 (FoxO1) plays an important role in processes associated with T2DM, such as insulin resistance, proliferation, differentiation, and apoptosis of islet β cells, and glucose and lipid metabolism [13–15]. The participation of FoxO1 in the regulation of blood glucose in osteoblasts has also been confirmed. Osteoblasts deficient in FoxO1 can reduce Esp expression and increase osteocalcin expression, thus increasing insulin sensitivity and insulin production [16].

In the present study, we hypothesized that FOXO1 and LCN2 are involved in the anti-diabetic effect of SG. The expressions of FOXO1 and LCN2 in bone were observed, and the binding rate of LCN2 and MC4R in the hypothalamus was measured after SG and sham surgeries, showing that FoxO1 is an upstream regulators of LCN2 in osteoblasts. The results suggest that the FOXO1/LCN2 signaling pathway is involved in the anti-diabetic effect of SG. Here, we present new insights into the mechanism by which metabolic surgery affects diabetes.

Material and Methods

T2DM animal models were established

Twenty male Wistar rats (55–60 days old, 200–220 g) were supplied by the Laboratory Animal Center of Shandong University (Jinan, China). The rats were maintained under the following conditions: room temperature 24–26°C, humidity 50–60%, and 12 h light/dark cycle. All rats were fed a high-fat diet (40% fat, Huafukang Biotech, China) for 4 weeks, then injected intraperitoneally with streptozotocin (30 mg/kg, Sigma Aldrich, USA) dissolved in sodium citrate buffer (pH=4.2) to induce a diabetic state after 12-h fasting. Rats with fasting blood glucose (FBG) ≥11.1 mmol/l stable for 14 days were used for research. Eighteen rats that were successfully induced to a diabetic state were randomly divided into the SG group (n=9) and sham group (n=9). The sham group underwent sham surgery to eliminate the effect of surgical stress on blood glucose. We gave 10% Ensure (Abbott Laboratories, USA) to rats for 48 h prior to surgery and 5 days after surgery. A high-fat diet (HFD) was continuously provided to the end of the experiment. All rats were euthanized by intravenous injection of a barbiturate overdose prior to collection of samples.

Surgery procedures

After 8 h of fasting, rats in the SG and sham groups were anesthetized by intraperitoneal injection of ketamine (75 mg/kg) [17,18].

In the SG group [19–21], a midline incision (approximately 4 cm) of the upper abdomen was made and the gastric omentum was dissected. Exploration of the abdominal cavity showed that none of the rats had gastrointestinal anomalies or intra-abdominal tumors. The cardia and the pylorus of the stomach

Indexed in: [Current Contents/Clinical Medicine] [SCI Expanded] [ISI Alerting System] [ISI Journals Master List] [Index Medicus/MEDLINE] [EMBASE/Excerpta Medica] [Chemical Abstracts/CAS]

were identified. Hemostatic forceps were used to clamp the maximum curvature from the cardia to the pylorus to prevent hemorrhage. The gastric omentum blood vessels were dissected and cut. Approximately 70% of the stomach outside the clamped area, including the fundus, was removed. After the sleeve gastrectomy was completed, the stomach incision was sutured with 7-0 silk suture (Ningbo Medical Needle, China). The abdominal wall was closed with 7-0 silk suture (Ningbo Medical Needle, China). Finally, 15 mL sterile saline was injected subcutaneously for postoperative hydration at the end of the procedure.

In the sham group [22], laparotomy was performed to expose the stomach and dissect the gastric omentum. The operation time was extended to mimic that of the SG group.

Glucose homeostasis was determined

FBG (mIU/L) and body weight (g) were measured twice a week. Serum samples were collected from the orbital vein. Fasting serum insulin (mIU/L) and HbA1c (%) were assessed before and after operations by enzyme-linked immunosorbent assay (ELISA). The oral glucose tolerance tests (OGTT) were performed at the 4th week after surgery [23]. After fasting for 8 h, the blood glucose levels of rats were measured at 0, 15, 30, 60, 90, and 120 min after glucose administration (1 g/kg). The glucometer was from Roche (Germany), and ELISA kits were from Wuhan USCN Business Co. (China).

Homeostatic model assessment-insulin resistance (HOMA-IR) and the area under the curve (AUC) of the OGTT were calculated. HOMA-IR=fasting insulin×FBG/22.5.

Tissues were processed and prepared.

Rats were sacrificed 4 weeks after surgery. The femur and hypothalamus were fixed in neutral buffered formalin for immunofluorescence assay. The femur was decalcified with EDTA for 1 month at room temperature. Then, the femur and hypothalamus were dehydrated and embedded to make paraffin sections.

Enzyme-linked immunosorbent assay (ELISA)

An LCN2 ELISA kit (CUSABIO Life Science, Wuhan, China) was used to detect fasting serum LCN2 before and after operations.

HE staining of femur and hypothalamus

HE staining was conducted according to routine protocols. The paraffin sections were immersed in xylene (Chinese Pharmaceutical Group, 10023418) and alcohol (Chinese Pharmaceutical Group, 100092683). After deparaffinization and rehydration, they were stained with hematoxylin solution (Google Biology, G1005) for 5 min, then stained with eosin (Google Biology, G1005) for 3 min and re-immersed in xylene and alcohol. The slides were mounted using neutral balsam (Chinese Pharmaceutical Group, 10004160) and photographed using a positive optical microscope (Nikon Eclipse CI, Japan).

Immunofluorescence of femur and hypothalamus

Femurs were dewaxed and antigen was repaired with a repair box filled with citric acid antigen repair buffer solution (G1202, Google Biology). The slides were washed in PBS (G0002, Google Biology) and sealed at 25°C for 30 min after drying. After the blocking solution was discarded, the primary antibody anti-LCN2 (ab63929, Abcam) or Foxo1 (GB11286) was added to the slides and incubated overnight at 4°C. For double immunofluorescent staining, hypothalami were incubated with anti-MC4R antibody (bs-11417R) overnight. After 24 h, the sections were washed and incubated with anti-LCN2 (ab63929, Abcam) for 2 h. Then, the slides were washed in PBS, and a secondary antibody, cy3-goat anti-rabbit (GB21303, Google Biology), was added dropwise. The slides were incubated at 25°C for 50 min and washed in PBS. DAPI (G1012, Google Biology) was added dropwise to slides and incubated at room temperature for 10 min. Finally, the slides were sealed with an anti-fluorescence quenching tablet (G1401, Google Biology).

Five immunofluorescence images were randomly captured on a Nikon Eclipse C1 confocal microscope at 400× magnification. Images were captured with a camera (Nikon DS-U3). Using Image J software, the expressions of LCN2 and FOXO1 in femurs were detected by calculating the mean of IOD in immunofluorescence images. To quantify the double immunofluorescence staining, the co-localization coefficient between LCN2 and MC4R was shown as the Pearson coefficient in the co-localization volume (1, completely correlated; 0, not correlated; –1, completely negatively correlated).

Cell Cultures

CP-R091 rat osteoblasts were purchased from Procell Life Cell Cultures Science & Technology Co. (Wuhan, China). Cells were cultured in osteoblast basal medium (CM-R091) as recommended by the supplier and maintained in a-minimal essential medium (a-MEM). The a-MEM (Gibco-BRL, Rockville, MD, USA) contained 1% (v/v) of penicillin/streptomycin and 10% (v/v) of heat-inactivated fetal bovine serum at 37°C in a humidified atmosphere of 95% air and 5% CO_2.

siRNA silencing

Lipofectamine RNAiMAX was used to transfect FOXO1 targeting siRNA or control (scrambled) siRNA into CP-R091 cells. FOXO1 silencing was achieved after 2 rounds of 100 nM siRNA

Indexed in: [Current Contents/Clinical Medicine] [SCI Expanded] [ISI Alerting System] [ISI Journals Master List] [Index Medicus/MEDLINE] [EMBASE/Excerpta Medica] [Chemical Abstracts/CAS]

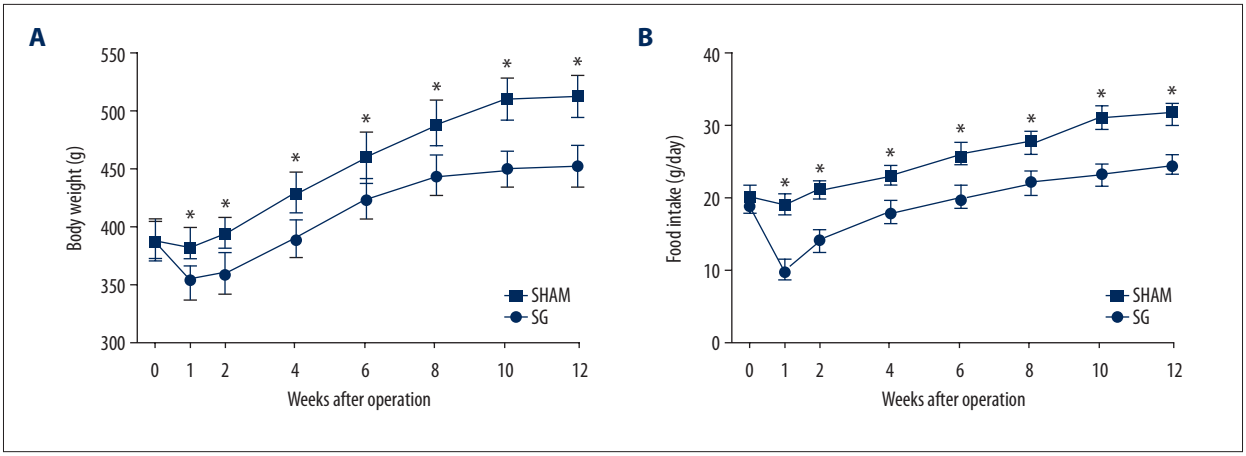

Figure 1. Body weight (**A**) and food intake (**B**) between SG and sham groups after operation, * p<0.05.

transfection. Western blot (WB) analysis and RT-qPCR were used to test the silencing efficiency of FOXO1. During the same period, the gene and protein levels of LCN2 were detected. The siRNA sequences were as follows:
5'-GCAAGUUUAUUCGAGUACAGA-3' (forward),
5'-UGUACUCGAAUAAACUUGCUG-3' (reverse).

WB

Cultured cells were lysed in RIPA buffer containing protease cocktail inhibitor. The phosphorylated protein was extracted using a phosphorylated protein extraction kit. The lysate was separated on SDS-polyacrylamide gel for electrophoresis. Then, the protein was transferred to the polyvinylidene fluoride membrane and incubated with primary anti-Foxo1 (GB11286, 1: 1000), anti-LCN2 (ab63929, 1: 1000), and anti-β-actin (GB12001, 1: 1000) at 4°C overnight. The membrane was incubated with a horseradish peroxidase-conjugated secondary antibody (Cell Signaling Technology, Beverly, MA, USA) for 1 h and was visualized using chemiluminescent reagents. Imaging was done using a gel imaging system (Tanon, Shanghai, China) and quantitative blotting was performed using Image J software.

RT-qPCR

Total RNA was isolated from osteoblasts using TRIzol reagent (G3013, Servicebio) and transcription was performed using the RevertAid First Strand cDNA Synthesis Kit (#K1622, Thermo). The reverse transcription condition was set at 65°C for 5 min, at 42°C for 60 min, and at 70°C for 5 min, with PCR amplification performed at the final stage. Analyses were performed on cDNA using FastStart Universal SYBR Green Master (04 913 914 001, Roche). All procedures were performed according to the manufacturer's instructions. The following primer pairs were used:
LCN2: 5'-AGCACCATCTATGAGCTACAGGA-3' (forward),
5'-CGAATGTTCTGATCCAGTAGCG-3'(reverse).
FoxO1: 5'- ACTTCAAGGATAAGGGCGACAG-3' (forward),
5'-ATTTCCCACTCTTGCCTCCCT-3'(reverse).
GAPDH: 5'-CTGGAGAAACCTGCCAAGTATG-3'(forward),
5'-GGTGGAAGAATGGGAGTTGCT-3'(reverse).

Statistical analysis

SPSS software (version 22.0) was used to analyze all statistical data. Graphpad Prism 8.0 software was used for drawing graphs. K-S and S-W tests were used in the normality test of measurement data. Combined with the data of P-P chart and Q-Q chart, the measurement data conforming to normal distribution were expressed in the form of mean±standard (x±s) deviation. The difference of measurement factors between the 2 groups was compared using a single-factor *t* test. Trapezoidal integration was used to calculate AUC of the OGTT. P<0.05 was considered as indicating a statistically significant difference.

Results

All surgeries were successfully conducted. One rat in the SG group died of stomach stump hemorrhage after the operation. No statistically significant difference was observed between the 2 groups before surgery (p > 0.05, data not shown).

SG surgery had a remarkable effect on reducing weight and improving glycometabolism

Body weight and food intake of the SG group were less than that of the sham group after operations (p<0.05, Figure 1). As shown in Figure 2A, there was a decrease in FBG levels in the SG group compared with the sham group after operations (p<0.05). The levels of fasting serum insulin were higher in the SG group compared with the sham group 4 weeks after surgery (p<0.05, Figure 2B). Levels of HOMA-IR and HbA1c were lower than those of the sham group 4 weeks after surgery (p<0.05,

Indexed in: [Current Contents/Clinical Medicine] [SCI Expanded] [ISI Alerting System] [ISI Journals Master List] [Index Medicus/MEDLINE] [EMBASE/Excerpta Medica] [Chemical Abstracts/CAS]

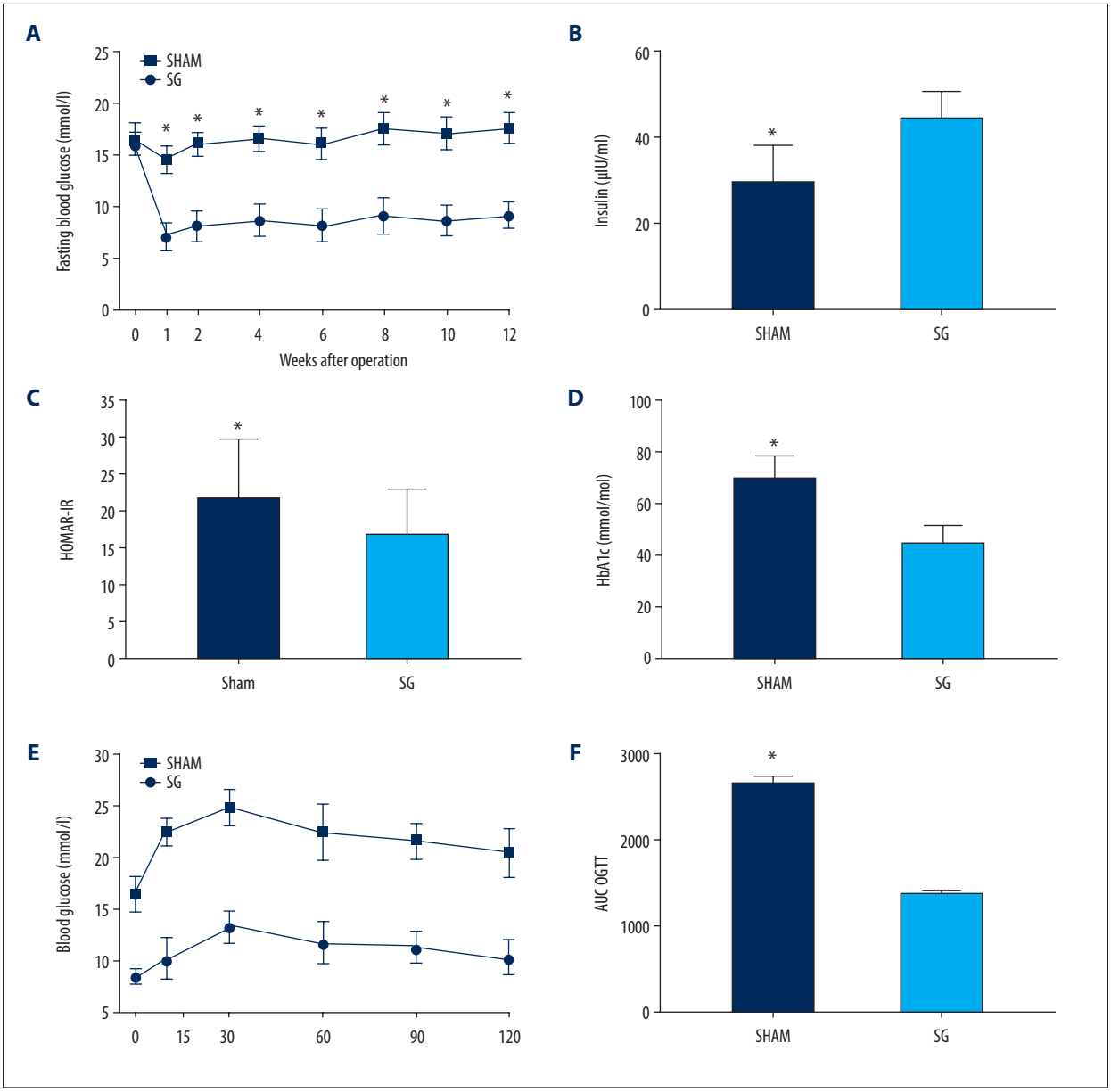

Figure 2. SG improved glycometabolism in rats with T2DM. (**A**) Fasting blood glucose of the 2 groups after surgery. (**B**) Fasting serum insulin levels of the 2 groups at the 4th week after surgery. (**C**) HOMO-IR of the 2 groups at the 4th week after surgery. (**D**) HbA1c of the 2 groups at the 4th week after surgery. (**E**) OGTT of the 2 groups at the 4th week after surgery. (**F**) The AUC of OGTT of the 2 groups at the 4th week after surgery. * p<0.05.

Figure 2C, 2D). The OGTT results of the 2 groups are presented in Figure 2E. The AUC of OGTT in the SG group was lower than in the sham group at 4 weeks after surgery (p<0.05, Figure 2F).

These results showed decreased glucose levels, increased insulin secretion, and improved insulin resistance after SG, indicating that SG had a significant anti-diabetic effect.

Serum LCN2 levels increased after SG

ELISA was used to evaluate the effect of SG on LCN2 levels in peripheral blood. Our results demonstrated that levels of fasting serum LCN2 in the SG group were higher than those in the sham group at 4 weeks after surgery (p<0.05, Figure 3), suggesting that SG increased LCN2 levels in peripheral blood.

Indexed in: [Current Contents/Clinical Medicine] [SCI Expanded] [ISI Alerting System] [ISI Journals Master List] [Index Medicus/MEDLINE] [EMBASE/Excerpta Medica] [Chemical Abstracts/CAS]

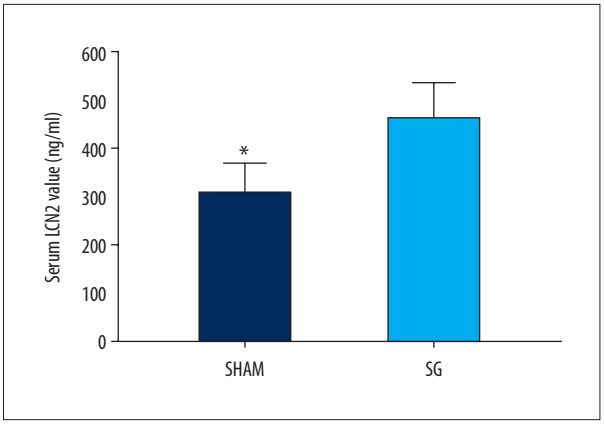

Figure 3. Fasting serum LCN2 levels of the 2 groups at the 4th week after surgery. * p<0.05.

HE staining of femur and hypothalamus

HE Staining was performed to observe the histomorphology of femurs and hypothalami (Figure 4). The area in the blue box of Figure 4A shows the position of the femoral osteoblasts. The area in the blue box of Figure 4B shows the position of the hypothalamus. The area in the blue box corresponds to the area detected by immunofluorescence.

LCN2 expression was higher and FOXO1 expression was lower in bone after SG

Bone is the main secretory organ of LCN2. Based on the analysis of LCN2 level in the peripheral blood after SG, we hypothesized that SG promotes the secretion of LCN2 in bone. Immunofluorescence was used to semi-quantitatively analyze the protein levels of LCN2 in femurs after SG, and the protein levels of FOXO1 in femurs were analyzed after SG. As shown in Figures 5, 6, LCN2 expression in the femur was higher in the

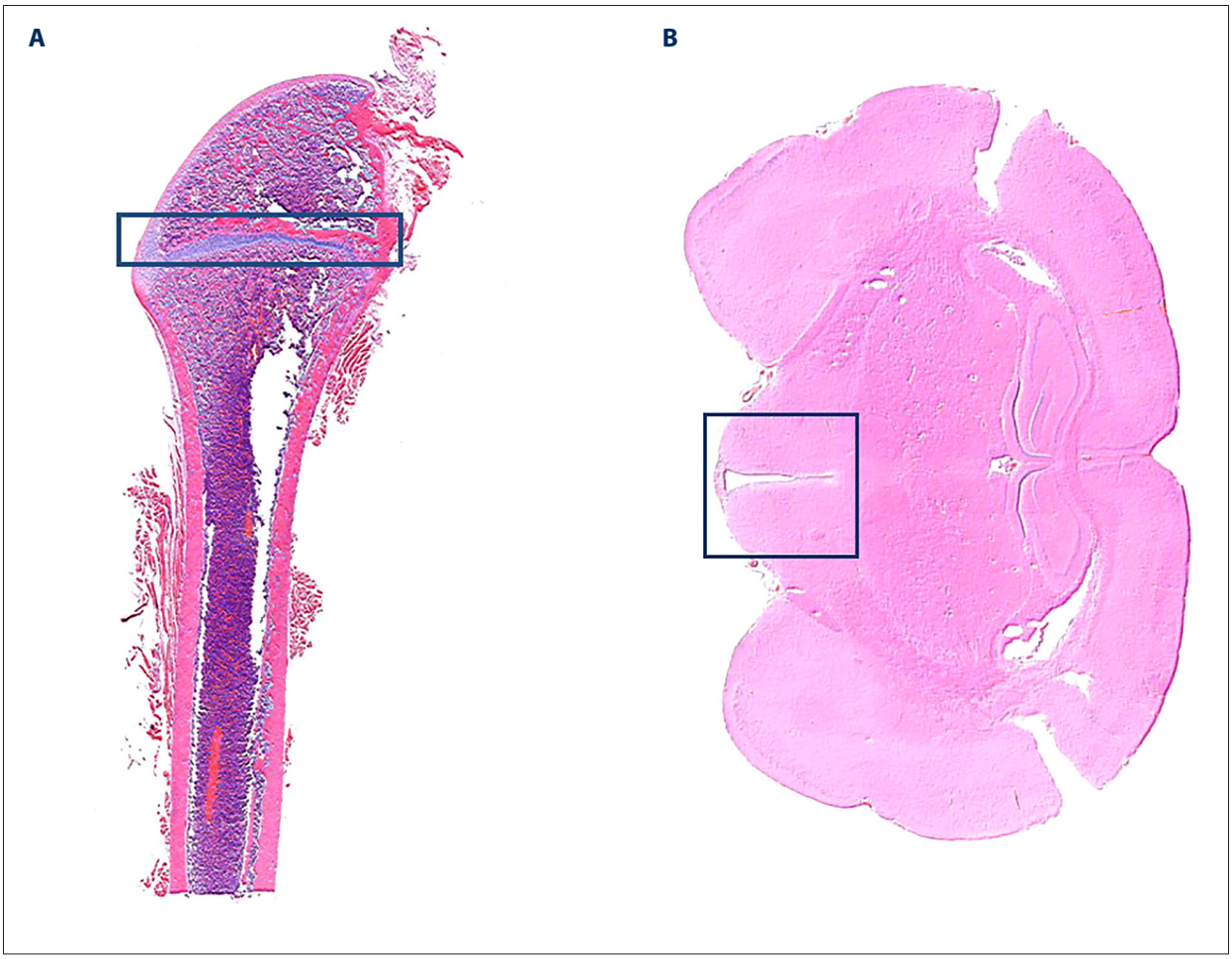

Figure 4. HE staining of femur and hypothalamus. The part in the blue box corresponds to the part detected by immunofluorescence. The area in the blue box of figure **A** is the position of the femoral osteoblasts. The area in the blue box of figure **B** is the position of the hypothalamus.

Indexed in: [Current Contents/Clinical Medicine] [SCI Expanded] [ISI Alerting System] [ISI Journals Master List] [Index Medicus/MEDLINE] [EMBASE/Excerpta Medica] [Chemical Abstracts/CAS]

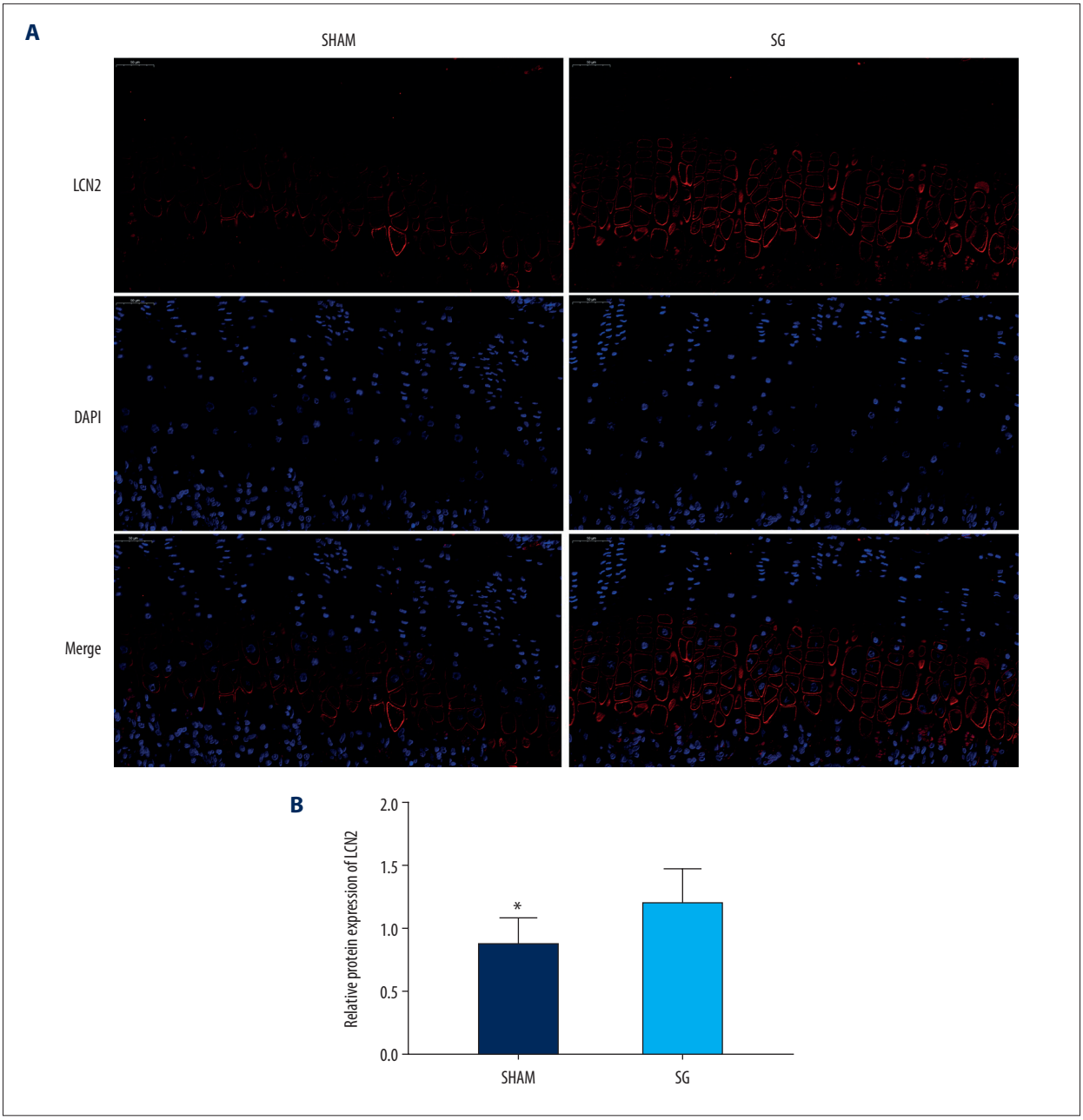

Figure 5. Effects of SG and sham surgeries on the expression of LCN2 in femur using immunofluorescence assays at the 4th week after surgery. (**A**) Immunofluorescence images showing the expression of LCN2. Red fluorescence indicates LCN2, while blue fluorescence indicates DAPI-labeled nuclei. Scale bar: 50 μm. (**B**) The bar graph showed quantitative analysis of LCN2. * $p<0.05$.

SG group than in the sham group, while FOXO1 expression in the femur was lower in the SG group compared with the sham group at 4 weeks after surgery ($p<0.05$). These results indicate that the expressions of LCN2 and FOXO1 in bone are affected by SG; therefore, we speculated that there is a correlation with the expression of LCN2 and FOXO1.

Binding of LCN2 and MC4R in the hypothalamus was enhanced after SG

To explore the effect of increased levels of LCN2 in the body after SG on energy metabolism, the binding rate of LCN2 and MC4R in the hypothalamus was tested by double immunofluorescent staining. As shown in Figure 7, double immunofluorescent staining using anti-MC4R (green) and anti-LCN2 (red)

Indexed in: [Current Contents/Clinical Medicine] [SCI Expanded] [ISI Alerting System] [ISI Journals Master List] [Index Medicus/MEDLINE] [EMBASE/Excerpta Medica] [Chemical Abstracts/CAS]

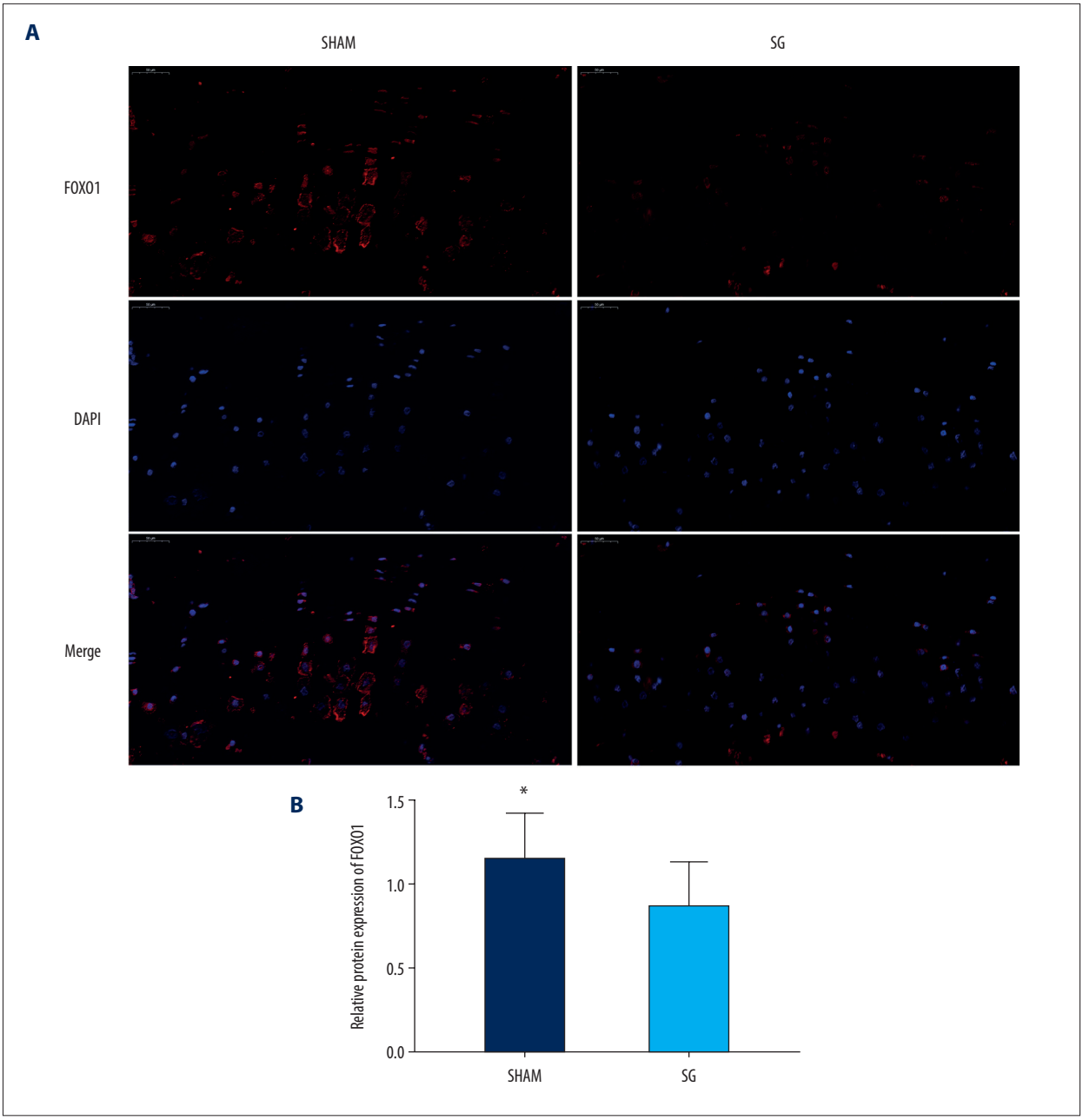

Figure 6. Effects of SG and sham surgeries on the expression of FOXO1 in femur using immunofluorescence assays at the 4th week after surgery. (**A**) Immunofluorescence images showing the expression of FOXO1. Red fluorescence indicates FOXO1, while blue fluorescence indicates DAPI-labeled nuclei. Scale bar: 50 μm. (**B**) The bar graph shows quantitative analysis of FOXO1. * $p<0.05$.

identified the binding rate of LCN2 and MC4R in the hypothalamus. The co-localization coefficient was used to semi-quantitatively analyze the binding rate. There was a significant increase in the co-localization coefficient of LCN2 and FOXO1 compared with that of the sham group after SG ($p<0.05$). This result indicates that SG enhanced the binding of LCN2 and MC4R in the hypothalamus.

Foxo1/LCN2 pathway exists in osteoblasts

Based on the analysis of the protein levels of LCN2 and FOXO1 in the bone after SG, we speculated that the decrease in FOXO1 levels after SG caused the increase in LCN2 levels. To confirm this speculation, we downregulated FOXO1 gene expression in osteoblasts through siRNA silencing technology and used RT-PCR and western blot to detect the gene and protein levels of

Indexed in: [Current Contents/Clinical Medicine] [SCI Expanded] [ISI Alerting System] [ISI Journals Master List] [Index Medicus/MEDLINE] [EMBASE/Excerpta Medica] [Chemical Abstracts/CAS]

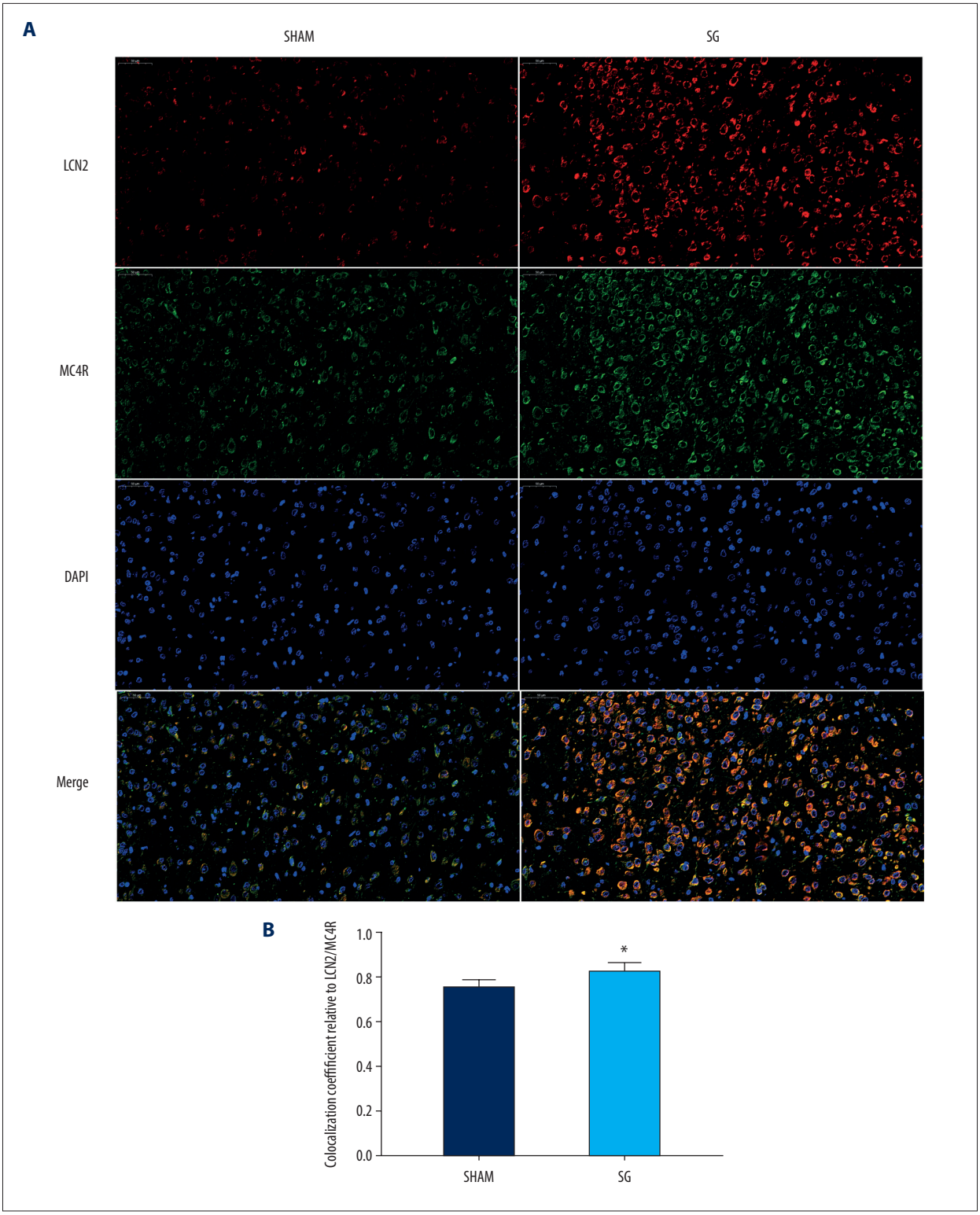

Figure 7. Effects of SG and sham surgeries on the expression of LCN2 and MC4R in hypothalamus using the double immunofluorescence assays at the 4th week after surgery. (**A**) Double immunofluorescence images showing the expression of LCN2 and MC4R. Red fluorescence indicated LCN2, green fluorescence indicated MC4R, blue fluorescence indicated DAPI-labeled nuclei. Scale bar: 50 μm. (**B**) The bar graph shows quantitative analysis of the co-localization coefficient between LCN2 and MC4R. * p<0.05.

Indexed in: [Current Contents/Clinical Medicine] [SCI Expanded] [ISI Alerting System] [ISI Journals Master List] [Index Medicus/MEDLINE] [EMBASE/Excerpta Medica] [Chemical Abstracts/CAS]

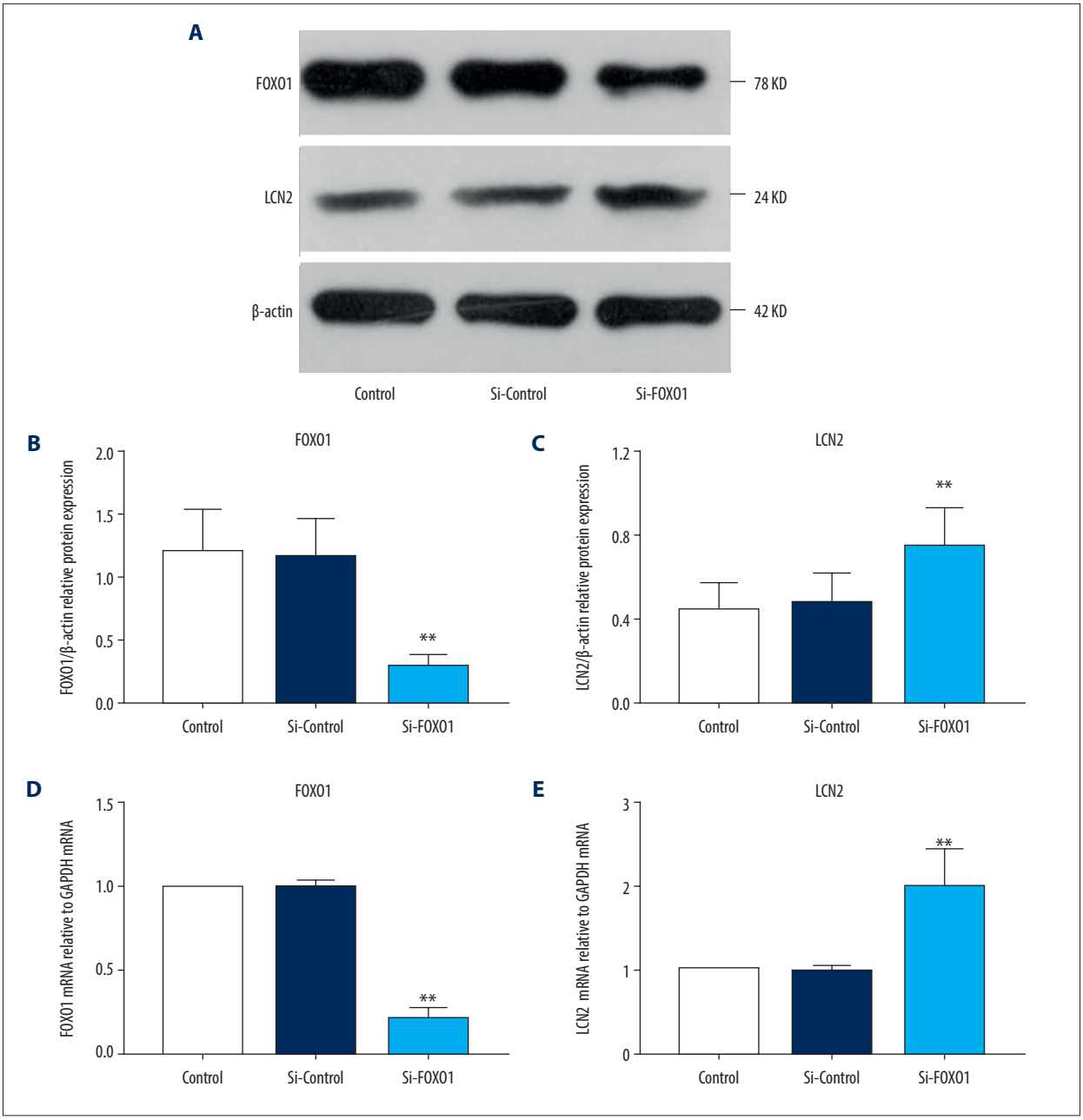

Figure 8. After downregulation of FOXO1 expression, the expression of LCN2 in osteoblasts at both the protein and mRNA levels. (**A–C**) Western blotting results of FOXO1 and LCN2. (**D, E**) RT-qPCR results of FOXO1 and LCN2. ** p<0.01.

LCN2 and FOXO1. With the downregulation of FOXO1 expression, the expression of LCN2 in osteoblasts at both the mRNA and protein levels was increased (p<0.01, Figure 8), showing that the Foxo1/LCN2 pathway exists in osteoblasts.

Discussion

Metabolic surgery has remarkable effects on reducing weight and improving glycometabolism [24,25]. Theories on the anti-diabetic effects of metabolic surgery have mainly focussed on increasing insulin secretion and decreasing insulin resistance in liver, muscle, and adipose tissues [18,26–28]. Bone has recently been recognized as a pleiotropic endocrine organ. A growing number of studies have shown that some bone-derived hormones that affect bone homeostasis affect glucose metabolism. These findings have shown that there may be a channel between the pancreas and bone to deal with metabolic and skeletal stress [7,11,29–31]. Among the hormones released by bone, FOXO1 and LCN2 can improve peripheral insulin sensitivity and

Indexed in: [Current Contents/Clinical Medicine] [SCI Expanded] [ISI Alerting System] [ISI Journals Master List] [Index Medicus/MEDLINE] [EMBASE/Excerpta Medica] [Chemical Abstracts/CAS]

modulate food intake and glucose homeostasis. Impaired FOXO1 or LCN2 can lead to disorders of energy homeostasis, resulting in a diet-induced obese phenotype in mice [12,16,32,33].

In the present study, bone immunofluorescence staining results showed that expression of FOXO1 was reduced and expression of LCN2 was increased in bone of diabetic rats after SG. FOXO1 is the main regulator of redox balance in osteoblasts. When high glucose induces an increase in oxidative stress, it can stimulate FOXO1 secretion [34–36]. Via integrated signals originating from the bone, FOXO1 can change the function and mass of pancreatic β cells. Some studies also found that insulin secretion and sensitivity can be regulated by FoxO1 in osteoblasts. Osteocalcin, an osteoblast-secreted hormone known to promote glucose homeostasis, can be upregulated by FoxO1 in osteoblasts [32,33,37–39].

Some data suggest that LCN2 is highly expressed in osteoblasts. After LCN2 gene knock-out in mice, the number of islet cells, β-cell function, and β-cell proliferation were all reduced, which ultimately causes a decrease in glucose tolerance and insulin sensitivity, leading to the occurrence of diabetes [12,40–42]. The effect of LCN2 on glucose tolerance might reflect its direct effect on islet cells. Mosialou et al. also found that the upregulation of LCN2 is a protective mechanism against glucose intolerance caused by obesity by reducing food intake and promoting adaptive β-cell proliferation. Osteoblast-derived LCN2 suppress appetite and reduce fat mass, while improving glucose metabolism [34]. Both FOXO1 and LCN2 can be secreted by osteoblasts, and can participate in regulation of glucose metabolism by affecting the mechanism of insulin resistance during the pathogenesis of diabetes. However, there are few reports on the interaction between FOXO1 and LCN2. In the present study, FOXO1 siRNA was applied to downregulate FOXO1 expression in osteoblasts of rats. After downregulation of FOXO1 expression in osteoblasts, expression of LCN2 was upregulated; therefore, we hypothesized that the FOXO1/LCN2 signaling pathway in bone is involved in the anti-diabetic effect of SG.

Studies have found that osteoblast-derived LCN2 can pass through the blood-brain barrier, combine with MC4R in the paraventricular and ventromedial neurons of the hypothalamus, activate the MC4R-dependent anorexia pathway, and then affect appetite and regulate liver glycogen output. In the present study, we found that the binding rate of LCN2 and MC4R in the hypothalamus was significantly increased after SG. It is generally believed that the pathogenesis of obesity and related diseases (such as diabetes and hypertension) is closely related to the regulatory role of the central nervous system [43–45]. The central melanocortin signaling pathway plays a key role, mainly by acting on MC4R. The interaction of arcuate proopiomelanocortin and neurons expressed with locus-related peptides can coordinate long-term energy homeostasis [46]. The loss of MC4R function can lead to development of obesity, insulin resistance, and diabetes [47]. MC4Rs are widely expressed in the central nervous system and are involved in energy balance regulation and sympathetic nerve outflow [48,49].

Conclusions

Our results suggest that the FOXO1/LCN2 signaling pathway in bone is involved in the anti-diabetic effect of metabolic surgery. This finding provides new insights into the mechanism of metabolic surgery and provides new ideas and directions for the treatment of obesity and DM.

Conflict of interest

None.

References:

1. Cho NH, Shaw JE, Karuranga S et al: IDF Diabetes Atlas: Global estimates of diabetes prevalence for 2017 and projections for 2045. Diabetes Res Clin Pract, 2018; 138: 271–81
2. Ren T, Ma A, Zhuo R, et al. Oleoylethanolamide Increases Glycogen Synthesis and Inhibits Hepatic Gluconeogenesis via the LKB1/AMPK Pathway in Type 2 Diabetic Model. J Pharmacol Exp Ther. 2020;373(1): 81-91.
3. Buchwald H, Avidor Y, Braunwald E et al: Bariatric surgery: A systematic review and meta-analysis. JAMA, 2004; 292(14): 1724–37
4. Angrisani L, Santonicola A, Iovino P et al: Bariatric surgery and endoluminal procedures: IFSO Worldwide Survey 2014. Obes Surg, 2017; 27(9): 2279–89
5. Blomain ES, Dirhan DA, Valentino MA et al: Mechanisms of weight regain following weight loss. ISRN Obes, 2013; 2013: 210524
6. Moore MC, Smith MS, Farmer B et al: Morning hyperinsulinemia primes the liver for glucose uptake and glycogen storage later in the day. Diabetes, 2018; 67(7): 1237–45
7. Bao Y, Ma X, Yang R et al: Inverse relationship between serum osteocalcin levels and visceral fat area in Chinese men. J Clin Endocrinol Metab, 2013; 98(1): 345–51
8. Aguirre L, Napoli N, Waters D et al: Increasing adiposity is associated with higher adipokine levels and lower bone mineral density in obese older adults. J Clin Endocrinol Metab, 2014; 99(9): 3290–97
9. Marino F, Tozzi M, Schembri L et al: Production of IL-8, VEGF and elastase by circulating and intraplaque neutrophils in patients with carotid atherosclerosis. PLoS One, 2015; 10(4): e0124565
10. Sood V, Bhansali A, Mittal BR et al: Autologous bone marrow derived stem cell therapy in patients with type 2 diabetes mellitus – defining adequate administration methods. World J Diabetes, 2017; 8(7): 381–89
11. Sanchez-Enriquez S, Ballesteros-Gonzalez IT, Villafán-Bernal JR et al: Serum levels of undercarboxylated osteocalcin are related to cardiovascular risk factors in patients with type 2 diabetes mellitus and healthy subjects. World J Diabetes, 2017; 8(1): 11–17
12. Mosialou I, Shikhel S, Liu JM et al: MC4R-dependent suppression of appetite by bone-derived lipocalin 2. Nature, 2017; 543(7645): 385–90
13. Zhang XQ, Xu CF, Yu CH et al: Role of endoplasmic reticulum stress in the pathogenesis of nonalcoholic fatty liver disease. World J Gastroenterol, 2014; 20(7): 1768–76
14. Kwon H, Pessin JE: Adipokines mediate inflammation and insulin resistance. Front Endocrinol (Lausanne), 2013; 4: 71

Indexed in: [Current Contents/Clinical Medicine] [SCI Expanded] [ISI Alerting System] [ISI Journals Master List] [Index Medicus/MEDLINE] [EMBASE/Excerpta Medica] [Chemical Abstracts/CAS]

15. Talchai SC, Accili D: Legacy effect of Foxo1 in pancreatic endocrine progenitors on adult β-cell mass and function. Diabetes, 2015; 64(8): 2868–79
16. Li N, Yan QT, Jing Q et al: Duodenal-Jejunal bypass ameliorates type 2 diabetes mellitus by activating insulin signaling and improving glucose utilization in the brain. Obes Surg, 2020; 30(1): 279–89
17. Hu C, Zhang G, Sun D et al: Duodenal-jejunal bypass improves glucose metabolism and adipokine expression independently of weight loss in a diabetic rat model. Obes Surg, 2013; 23(9): 1436–44
18. Hu C, Su Q, Li F et al: Duodenal-Jejunal bypass improves glucose homeostasis in association with decreased proinflammatory response and activation of JNK in the liver and adipose tissue in a T2DM rat model. Obes Surg, 2014; 24(9): 1453–62
19. Ferhatoglu MF, Kıvılcım T, Senol K et al: The positive effects of the human amniotic membrane on the healing of staple line after sleeve gastrectomy applied long-evans rat model. Obes Surg, 2019; 29(11): 3560–68
20. Sun D, Liu S, Zhang G et al: Sub-sleeve gastrectomy achieves good diabetes control without weight loss in a non-obese diabetic rat model. Surg Endosc, 2014; 28(3): 1010–18
21. Pereferrer FS, Gonzàlez MH, Rovira AF et al: Influence of sleeve gastrectomy on several experimental models of obesity: Metabolic and hormonal implications. Obes Surg, 2008; 18(1): 97–108
22. Bruinsma BG, Uygun K, Yarmush ML, Saeidi N: Surgical models of Roux-en-Y gastric bypass surgery and sleeve gastrectomy in rats and mice. Nat Protoc, 2015; 10(3): 495–507
23. Cheng Y, Huang X, Wu D et al: Sleeve gastrectomy with bypass of proximal small intestine provides better diabetes control than sleeve gastrectomy alone under postoperative high-fat diet. Obes Surg, 2019; 29(1): 84–92
24. Pareek M, Schauer PR, Kaplan LM et al: Metabolic surgery: Weight loss, diabetes, and beyond. J Am Coll Cardiol, 2018; 71(6): 670–87
25. Cummings DE, Cohen RV: Bariatric/metabolic surgery to treat type 2 diabetes in patients with a BMI <35 kg/m^2. Diabetes Care, 2016; 39(6): 924–33
26. Batterham RL, Cummings DE: Mechanisms of diabetes improvement following bariatric/metabolic surgery. Diabetes Care, 2016; 39(6): 893–901
27. Kuhre RE, Wewer Albrechtsen NJ, Larsen O et al: Bile acids are important direct and indirect regulators of the secretion of appetite- and metabolism-regulating hormones from the gut and pancreas. Mol Metab, 2018; 11: 84–95
28. Li M, Li H, Zhou Z et al.: Duodenal-Jejunal bypass surgery ameliorates glucose homeostasis and reduces endoplasmic reticulum stress in the liver tissue in a diabetic rat model. Obes Surg, 2016; 26(5): 1002–9
29. De Pergola G, Triggiani V, Bartolomeo N et al: Independent relationship of osteocalcin circulating levels with obesity, type 2 diabetes, hypertension, and HDL cholesterol. Endocr Metab Immune Disord Drug Targets, 2016; 16(4): 270–75
30. Schlecht I, Fischer B, Behrens G, Leitzmann MF: Relations of visceral and abdominal subcutaneous adipose tissue, body mass index, and waist circumference to serum concentrations of parameters of chronic inflammation. Obes Facts, 2016; 9(3): 144–57
31. De la Chesnaye E, Manuel-Apolinar L, Zarate A et al: Lipocalin-2 plasmatic levels are reduced in patients with long-term type 2 diabetes mellitus. Int J Clin Exp Med, 2015; 8(2): 2853–59
32. Boal F, Timotin A, Roumegoux J et al: Apelin-13 administration protects against ischaemia/reperfusion-mediated apoptosis through the FoxO1 pathway in high-fat diet-induced obesity. Br J Pharmacol, 2016; 173(11): 1850–63
33. Guo W, Jiang T, Lian C et al: QKI deficiency promotes FoxO1 mediated nitrosative stress and endoplasmic reticulum stress contributing to increased vulnerability to ischemic injury in diabetic heart. J Mol Cell Cardiol, 2014; 75: 131–40
34. Qian K, Tan T, Ouyang H et al: Structural characterization of a homopolysaccharide with hypoglycemic activity from the roots of *Pueraria lobata*. Food Funct, 2020 [Online ahead of print]
35. Yao Q, Zhou Y, Yang Y et al: Activation of Sirtuin1 by lyceum barbarum polysaccharides in protection against diabetic cataract. J Ethnopharmacol, 2020; 261: 113165
36. Yuan H, Li Y, Ling F et al: The phytochemical epigallocatechin gallate prolongs the lifespan by improving lipid metabolism, reducing inflammation and oxidative stress in high-fat diet-fed obese rats. Aging Cell, 2020 [Online ahead of print]
37. He Y, Cao X, Guo P et al: Quercetin induces autophagy via FOXO1-dependent pathways and autophagy suppression enhances quercetin-induced apoptosis in PASMCs in hypoxia. Free Radic Biol Med, 2017; 103: 165–76
38. Liu Q, Zhang FG, Zhang WS et al: Ginsenoside Rg1 inhibits glucagon-induced hepatic gluconeogenesis through Akt-FoxO1 interaction. Theranostics, 2017; 7(16): 4001–12
39. Lee NK, Sowa H, Hinoi E et al: Endocrine regulation of energy metabolism by the skeleton. Cell, 2007; 130(3): 456–69
40. Zhang Y, Liu M, Chen H et al: Associations between circulating bone-derived hormones lipocalin 2, osteocalcin, and glucose metabolism in acromegaly. J Endocrinol Invest, 2020; 43(9): 1309–16
41. Currò D, Vergani E, Bruno C et al: Plasmatic lipocalin-2 levels in chronic low-grade inflammation syndromes: Comparison between metabolic syndrome, total and partial adult growth hormone deficiency. Biofactors, 2020 [Online ahead of print]
42. Mera P, Ferron M, Mosialou I: Regulation of energy metabolism by bone-derived hormones. Cold Spring Harb Perspect Med, 2018; 8(6): a031666
43. Yang Z, Liang XF, Li GL, Tao YX: Biased signaling in fish melanocortin-4 receptors (MC4Rs): Divergent pharmacology of four ligands on spotted scat (*Scatophagus argus*) and grass carp (*Ctenopharyngodon idella*) MC4Rs. Mol Cell Endocrinol, 2020 [Online ahead of print]
44. Nyamugenda E, Griffin H, Russell S et al: Selective survival of Sim1/MC4R neurons in diet-induced obesity. iScience, 2020; 23(5): 101114
45. Hammad MM, Abu-Farha M, Hebbar P et al: MC4R Variant rs17782313 associates with increased levels of DNAJC27, ghrelin, and visfatin and correlates with obesity and hypertension in a Kuwaiti cohort. Front Endocrinol (Lausanne), 2020; 11: 437
46. Yu J, Gimenez LE, Hernandez CC et al: Determination of the melanocortin-4 receptor structure identifies Ca2+ as a cofactor for ligand binding. Science, 2020; 368(6489): 428–33
47. Xiao C, Liu N, Province H et al: BRS3 in both MC4R- and SIM1-expressing neurons regulates energy homeostasis in mice. Mol Metab, 2020; 36: 100969
48. Sutton AK, Gonzalez IE, Sadagurski M et al: Paraventricular, subparaventricular and periventricular hypothalamic IRS4-expressing neurons are required for normal energy balance. Sci Rep, 2020; 10(1): 5546
49. Paisdzior S, Dimitriou IM, Schöpe PC et al: Differential signaling profiles of MC4R mutations with three different ligands. Int J Mol Sci, 2020; 21(4): 1224

Indexed in: [Current Contents/Clinical Medicine] [SCI Expanded] [ISI Alerting System] [ISI Journals Master List] [Index Medicus/MEDLINE] [EMBASE/Excerpta Medica] [Chemical Abstracts/CAS]